Phonon transport in pressure-made point contacts

1998 J. Phys.: Condens. Matter 10 8313

(http://iopscience.iop.org/0953-8984/10/37/017)

J. Phys.: Condens. Matter **10** (1998) 8313–8326. Printed in the UK PII: S0953-8984(98)91457-6

Phonon transport in pressure-made point contacts

A G Shkorbatov†, P Štefányi‡, E Bystrenová‡ and A Feher‡

† B Verkin Institute for Low Temperature Physics and Engineering, National Academy of Science of Ukraine, 47 Lenin Avenue, 310164, Kharkov, Ukraine

‡ P J Šafárik University, park Angelinum 9, SK-04 154 Košice, Slovakia

Received 9 February 1998

Abstract. A theoretical and experimental analysis of the heat conductivity in metal–dielectric point contacts is given. The contribution of the phonon diffraction effects to the heat conductivity is investigated. The phonon heat transport through the point contacts is measured from 0.1 K to 100 K using the anvil–needle technique. In KBr–KBr and KBr–Cu point contacts, substituting a Cu needle for the dielectric cold edge does not disturb the heat conductivity pattern. Measurements for Si–Cu point contacts reveal well-defined diffraction maxima of reduced heat conductivity at temperatures in the range 0.5 K–1 K.

1. Introduction

Point contacts (PCs) with dimensions smaller than the scattering length of the charge and heat carriers have been intensively investigated in recent years [1]. First, conductive PCs with ballistic electron conductivity were studied [2, 3]. The non-linearity of the current–voltage characteristics of such contacts is the basis of the point-contact spectroscopy of phonon states in metals [4].

A variety of techniques were developed to obtain PCs [1]. The spear–anvil [5], cross-wedge [6, 7] and break-junction [8, 9] techniques are suitable for the investigation of electron and phonon transport in PCs. In PCs, electrons and phonons cannot flow through the surface to the vacuum outside of the contact.

The specific character of transport phenomena in point contacts is governed by how easy it is to create a strongly non-equilibrium state of the electron–phonon system in the constriction region. In a traditional treatment [1], one just applies a potential difference to the edges of the contact. In this case the electron system usually turns out to be strongly non-equilibrium. The phonon system is slightly excited, to the extent of undergoing some degree of interaction with the electrons, which is usually rather small in the contact. Like applying a voltage, keeping the edges at different temperatures can also change the situation significantly. If a temperature difference is established across the contact, the phonon system becomes strongly non-equilibrium, too.

A non-equilibrium phonon system can be realized in PCs if the size of the contact (d) is small compared with the phonon–phonon relaxation length ($l_{\mathrm{ph-ph}}$). Ballistic phonon transport arises in PCs if the phonon quasimomentum relaxation length (l) is large compared to the contact diameter (d).

In this paper we consider the situation in which the bulk edges of the contact are kept at different temperatures, T_2 and T_1. The peculiarity of such contacts is the existence of phonon and electron groups in the region of the contact whose distribution functions are

0953-8984/98/378313+14$19.50

characterized by different temperatures T_2 and T_1. An average temperature in the contact cannot be established because the degree of non-elastic interaction is small ($d \ll l_{\mathrm{ph-ph}}$).

We shall begin with a brief theoretical consideration of ballistic transport of phonons in dielectric point contacts, and then we shall gradually take into account the influence of different mechanisms of phonon scattering.

In this paper we present an application of a technique based on highly stable point contacts; it involves using metal–dielectric point contacts. The low-temperature heat conductivity data give clear pictures of the phonon diffraction in PCs, from which estimates of the point-contact-geometry parameters can be obtained. We show that the preparation of PCs by applying pressure gives rise to a polycontact structure of the contact region when the heat conduction between contacting edges is realized through a number of parallel PCs.

Different regimes of the heat conductivity were obtained by varying the pressure applied to the contact. If the pressure is insufficient to produce stable polycontacts, the contact through some of the weak junctions is lost when the temperature increases. On the other hand, in the stable PCs produced by applying higher pressure, additional phonon scattering results from the substrate lattice distortions in the contact region.

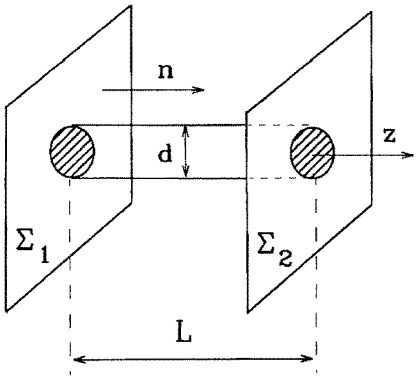

Figure 1. A schematic diagram of a point contact in the form of a cylindrical short-circuit in the vacuum gap between two surfaces.

2. Ballistic phonon transport in point contacts

2.1. The geometrical optics approximation

We model the point contact between two dielectrics as a short bridge (figure 1), whose dimensions are all small compared with the phonon–phonon and phonon–impurity scattering lengths in a bulk sample. When the contact size (d or L, where L is the contact length, as shown in figure 1) does not exceed 100 nm, this condition is as a rule easily met at low temperatures that are small in comparison with the Debye temperature Θ_D. In this section, the dimensions of the contact are assumed to be macroscopic relative to the characteristic elastic phonon wavelength λ (the geometrical optics approximation).

It is assumed that the bulk edges of the contact are at different temperatures, T_2 and T_1. A distinctive feature of the ballistic regime of the phonon transport in such a point contact is that phonons with temperatures T_2 and T_1 will exist in the region of the contact. Because no collisions occur in the contact, an average temperature cannot be established.

The system of equations describing the phonons in a dielectric PC consists of a kinetic equation for the distribution function of the phonons, $N(\boldsymbol{k}, \boldsymbol{r})$ ($\boldsymbol{k}$ is phonon wave vector, $\boldsymbol{r}$ is the point to which the phonon distribution function N is related), and boundary conditions,

which take into account the difference between the temperatures in the two contact edges and the phonon transport in the contact interface.

Since the heat transport in the dielectric PCs is realized through two non-interacting phonon groups whose distribution functions are determined by the temperatures T_2 and T_1 of the bulk edges of the contact, the ballistic heat flux $\dot{Q}_B(T_2, T_1)$ carried by the phonons can be represented by the relation [10]

$$\dot{Q}_B(T_2, T_1) = \frac{\hbar S_0}{2(2\pi)^3} \sum_\alpha \int_{u_z^\alpha > 0} \mathrm{d}\boldsymbol{k}\ \omega^\alpha(\boldsymbol{k}) |\boldsymbol{u}_z^\alpha| D_{12}^\alpha [N_2(\omega^\alpha(\boldsymbol{k}), T_2) - N_1(\omega^\alpha(\boldsymbol{k}), T_1)]. \qquad (1)$$

Here S_0 is the contact area, the z-axis is normal to the contact plane, $\boldsymbol{k}$ is the phonon wave vector, $\omega(\boldsymbol{k})$ is the frequency–wave-vector relation for phonons, $\boldsymbol{u} = \partial\omega(\boldsymbol{k})/\partial\boldsymbol{k}$ is the group velocity, and α is the phonon spectral branch index.

If the phonon distribution functions at the bulk edges are equilibrium functions, we should put

$$N_1 = n_P(\omega, T_1) = [\mathrm{e}^{(\hbar\omega/T_1)} - 1]^{-1} \qquad N_2 = n_P(\omega, T_2) = [\mathrm{e}^{(\hbar\omega/T_2)} - 1]^{-1}$$

where n_P is the Planck distribution function. Equation (1) contains the coefficient $D_{12}(\boldsymbol{k})$ of the phonon energy transfer from edge 1 to edge 2, and $\omega(\boldsymbol{k})$ is the expression for edge 1.

The coefficient $D_{12}^\alpha(\boldsymbol{k})$ is determined by the properties of the crystal lattices of the edges, and can be calculated by considering the problem of transfer of an elastic plane wave through the infinite planar interface of the two media [11, 12]. The incident plane wave in edge 1 produces, at the contact interface, three excited wave modes of index β in the edge 2. We should consider $D_{12}^\alpha(\boldsymbol{k})$ as a sum over these branches. Note that in equation (1) the frequency $\omega(\boldsymbol{k})$ and $D_{12}^\alpha(\boldsymbol{k})$ are for the arbitrary edge 1. This representation is valid owing to the useful reciprocity theorem for phonon transitions at ideal interfaces [12]. This theorem states that the power transition coefficient is the same for the direct transition from the wave mode α in edge 1 to the wave mode β in edge 2 (that is, $1, \alpha \Rightarrow 2, \beta$) as for the reverse transition (that is, $2, \alpha \Rightarrow 1, \beta$).

In the low-frequency region, for which a model of acoustic mismatch [11] can be used, $D_{12}^\alpha(\boldsymbol{k})$ does not actually depend on the frequency. In the case of the contact of two identical media, one should choose $D_{21}^\alpha(\boldsymbol{k}) = 1$ in the geometrical optics approximation.

At low temperatures, only the low-frequency oscillations are excited, and the frequency can be represented in the linear approximation: $\omega(\boldsymbol{k}) = \boldsymbol{u} \cdot \boldsymbol{k}$, and for the heat flux we get

$$\dot{Q}_B(T_2, T_1) = \frac{\pi^2 S_0 k_B}{120\hbar^3}(T_2^4 - T_1^4) \sum_\alpha (u^\alpha)^{-2} D_{12}^\alpha. \qquad (2)$$

The behaviour of the point-contact heat flux at low temperatures is similar to that obtained by Khalatnikov [13] and Little [11], who dealt with the thermal resistance between two media. The temperature jump can be realized not only in point contacts, but also in systems in which the phonon scattering at the boundary between two media is stronger than the thermal resistance in the bulk [14]. Such an effect was observed for the first time in Kapitza's experiments on heat exchange between superfluid helium and bulk metal [15]. It should be noted that the presence of two media is not required for the formation of a point-contact temperature jump. It can be stated that this jump emerges due to the scattering of phonons at the boundaries of the vacuum gap forming the point contact.

The low-temperature dependence $\dot{Q}(T_2, T_1) \sim T^4$ may serve as an experimental criterion for the realization of the geometrical optics approximation for the ballistic transport of phonons in point contacts.

Model calculations for two fcc lattices in contact [16] show that the simple T^4-law should be valid for the heat flux even if the temperature approaches the region in which

the Debye approximation can be applied. However, the thermal conductivity of real point contacts can depend upon the temperature in a more complicated way.

2.2. The diffraction regime of phonon transport

Low-temperature experiments [17] show that, as a rule, the temperature dependence of $\dot{Q}(T_2, T_1)$ has a complex form:

$$\dot{Q}(T_2, T_1) \sim F(T)(T_2^4 - T_1^4) \tag{3}$$

where the function $F(T)$ has a sharp peak at $T \sim 1$ K. Since this phenomenon also occurs in homogeneous contacts between identical materials, it can naturally be assumed that the low-temperature anomalies appear due to violation of the geometrical optics condition ($d \gg \lambda$). Indeed, since the characteristic wavelength of phonons at a temperature T can be estimated as $\lambda = a\Theta_D/T$ (a is the lattice constant), we can easily obtain the value of the temperature T_{dif} at which the condition $d \sim \lambda$ is satisfied: $T_{dif} \sim \Theta_D a/d$. For a contact of size $d \sim 102$ nm, we obtain $T_{dif} \sim 0.1$–1 K. At T_{dif} and at lower temperatures, we cannot consider phonon transport in the geometrical optics limit, since the diffraction of elastic waves at the point contact becomes significant.

Let us consider the ratio of the energy fluxes with and without the diffraction effect as the energy-transfer coefficient $D(k)$ in a homocontact. We calculate the energy flux in the approximation of a continuous isotropic medium, considering harmonic oscillations of the displacement vector $\boldsymbol{u}(\boldsymbol{r})\mathrm{e}^{-\mathrm{i}\omega t}$ (where t is the time) under the condition $|\boldsymbol{u}| \Rightarrow 1$ if $r \Rightarrow \infty$. In the simplest case of an isotropic medium, the elastic modulus tensor is defined by the velocities of the transverse and longitudinal waves. In the case of normal incidence of waves at the contact aperture, the conversion of phonon branches does not occur, and the energy-transfer coefficient $D(k)$ averaged over the period of oscillation can be written in the form (we omit the branch index)

$$D(k) = (S_0 k)^{-1} \int \mathrm{d}\boldsymbol{S}_0 \ \mathrm{Im}(u_k^*(\boldsymbol{r})\, \nabla u_k(\boldsymbol{r})). \tag{4}$$

The amplitude u satisfies the wave equation

$$-\nabla u_k(\boldsymbol{r}) = k^2 u_k(\boldsymbol{r}). \tag{5}$$

Here the subscript $\boldsymbol{k}$ corresponds to the solution of the equation for an incident plane wave with wave vector $\boldsymbol{k}$.

It is convenient to present the solution of the wave equation as a sum of normal modes corresponding to the boundary conditions. In the case of three-dimensional contact, the expression for the energy-transport coefficient averaged over $\boldsymbol{k}$-vector orientations is [18]

$$D^{\alpha}(k) = \left(\frac{4}{kd}\right)^2 \sum_{\mu,\nu} T^{\alpha}_{\mu,\nu}(k). \tag{6}$$

The transition probability $T^{\alpha}_{\mu,\nu}(k)$ of the propagating mode (μ, ν) is in the form of a step in the interval $0 \leqslant T \leqslant 1$. The sum runs over the total number of modes. The mode transmission through the contact ($T^{\alpha}_{\mu,\nu}(k) \Rightarrow 1$) occurs approximately each time the parameter kd increases by 2. This result is analogous to Landauer's formula [19] for the electric conductance of a ballistic contact.

The boundary condition for wave reflection at free surfaces forming the contact is significant. Under elastic reflection, the Neumann-type condition admits non-zero values of the displacement at the contact surface [18]. For planar contact geometry, the variation principle applicable to Neumann's problem leads to almost complete transmission of the

wave through the aperture [20]. A contact in the form of a channel with absolutely rigid walls is simulated using the 'spherical flow' model [21]. If the frequency of the incident wave coincides with the frequencies of the longitudinal vibrations of the channel, the result is an effective transmission of the wave energy at the resonant frequency ω_R of order $\pi u/L$. In the case of a channel with absolutely rigid walls, which satisfies the Neumann condition, the energy-transmission coefficient $D(k)$ has a number of diffraction maxima [18]. The low-frequency maximum at $k \sim \pi/L$ is of the largest amplitude. The value of the temperature T_{dif} at which the diffraction effect leads to increasing of the point-contact heat conductivity is of order $\Theta_D a/L$.

A strong attenuation of the waves at the contact surface can be described by requiring that the displacement at the surface be equal to zero (Dirichlet's condition). Apertures [22–24] and channels with wave attenuation at the surface [25–27] have been studied in great detail in connection with the problem of quantum-mechanical ballistic transport of electrons in contacts. Since low-frequency oscillations cannot propagate in these channels for $k < 1/d$, the effective energy transmission does not appear in this case.

For the thermal flux through the contact, neglecting the branch conversion, we obtain from (1) and (6)

$$\dot{Q}(T_2, T_1) = \left(\frac{\hbar}{2\pi}\right) \sum_{\alpha} \int_0^{\infty} \omega \, \mathrm{d}\omega \, t^{\alpha}(\omega)[N_2(\omega, T_2) - N_1(\omega, T_1)] \tag{7}$$

where $t^{\alpha}(\omega)$ is the sum over normal oscillations:

$$t^{\alpha}(\omega) = \sum_{\mu,\nu} T^{\alpha}_{\mu,\nu}(k(\omega)). \tag{8}$$

In the limiting case in which the thermal flux is transported by monochromatic phonons with distribution $N_1(\omega) = n\delta(\omega - \omega_0)$ (where n is a coefficient, ω is the current phonon frequency and ω_0 is the fixed monochromatic phonon frequency) and $N_2 = 0$, we arrive at the simple formula

$$\dot{Q}(T_2, T_1) = n\left(\frac{\hbar\omega_0}{2\pi}\right) \sum_{\alpha} \sum_{\mu,\nu} T^{\alpha}_{\mu,\nu}(k(\omega_0)). \tag{9}$$

Here, the subscripts μ and ν are the numbers of transverse vibration modes in a contact. Note that in this simple case the phonon heat flux is quantized in units of $\hbar\omega_0/2\pi$.

Figure 2 shows the result of the reduced-phonon-energy-flux calculation in the 'spherical flow' model for a contact with absolutely rigid walls. The lattice is assumed to be cubic.

3. Phonon scattering in point contacts

3.1. Phonon–lattice-distortion scattering

The review presented by Swartz and Pohl [14] leads to the conclusion that phonon scattering by structural imperfections in the lattice near the contact interface can result in a T^x-law, where $x < 4$ for low-temperature phonon flow. The interface disorder can play a role in the point-contact heat conductivity [28].

We can estimate the extent of departure from the ballistic regime and analyse the phonon scattering mechanism in the contact by assuming that the phonon transport becomes diffusive with an effective phonon quasimomentum scattering length $l(T) < d$. In this case, the thermal flux through the contact decreases by a factor l/d as compared to that in the ballistic regime. A more realistic model takes into consideration the fact that the phonon scattering lengths may be different at different edges of the contact (l_1 and l_2 respectively,

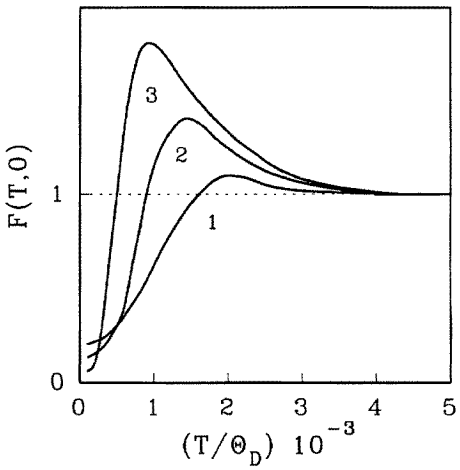

Figure 2. The reduced-phonon-energy-flux calculation in the 'spherical flow' model for a contact with an absolutely rigid surface. The contact diameter $d = 32a$, where a is the lattice constant. The length-to-diameter ratio of the contact, L/d, takes the values 1.5 (1), 2.5 (2) and 5 (3).

and analogous lengths for the contact edges). Considering the energy balance of the phonon transport across the contact interface under the assumption of elastic phonon scattering, we can find the correction factor G for the integral in formula (1) for the thermal flux, which describes the transition to the diffusive regime:

$$G^{\alpha} = \frac{32}{3\pi} d^{-1} \left(\frac{D_{12}^{\alpha}}{l_1^{\alpha}} + \frac{D_{21}^{\alpha}}{l_2^{\alpha}} \right)^{-1}. \tag{10}$$

Here D_{12} and D_{21} are the phonon energy-transfer coefficients averaged over $\boldsymbol{k}$-vector orientations.

3.2. Phonon–electron scattering in metal–dielectric PCs

If a metallic needle is used as one of the edges, the effect of the electronic system of the metal on the heat transfer in a PC has to be analysed [29]. The electron mechanism of heat transfer in PCs works only in the thermal bottleneck situation, where heat removal by phonons is hampered. When the phonon transport is not ballistic, multiple phonon–electron scattering should be included. We denote by T_d and T_m the temperatures of the dielectric and metallic edges, respectively. In our problem, T_m denotes the temperatures of the phonon and electron systems of the bulk metal, which are equal because a small heat flux through the PC cannot disturb this equality. Suppose that the phonon transport in a metallic edge is hampered due to the small elastic relaxation length l_m of the phonon quasimomentum ($l_m < d$).

If we assume that, owing to sufficiently high acoustic impedance of the metal, $D_d/l \ll D_m/l_m$, and consider the case where $T_d \gg T_m = 0$, we arrive at the expression for the phonon heat flux $\dot{Q}_{dm}$ in metal–dielectric PCs:

$$\dot{Q}_{dm}(T_d, 0) = \dot{Q}(T_d, 0) \left[1 + \frac{d}{l_a(T_d)} \right]. \tag{11}$$

Here the length l_a has a clear geometric meaning: there is an l_a-wide region at the metallic edge within which the injected phonons are attenuated, and $\dot{Q}$ is the flux in dielectric–

dielectric PCs of similar acoustic properties. Equation (11) shows the phonon–electron contribution to the phonon flux. This characteristic inelastic phonon attenuation length is determined by the phonon–electron scattering length $l_{\mathrm{ph-e}}(T_d) = a\varepsilon_F/T_d \gg d$ (where ε_F is Fermi energy of the metal), and l_m:

$$l_a = (l_{\mathrm{ph-e}} l_m)^{1/2}. \tag{12}$$

Equation (11) is for the realistic case of a weak bulk attenuation of phonons, when $l_m < d < l_a$. In this case, the contribution of the bulk phonon–electron scattering does not affect the heat conductivity of a PC. This result is important, because it enables us to study solely the mechanism of phonon heat transport, with the help of metal–dielectric PCs.

3.3. Phonon–phonon scattering in a point contact

The common scheme for the analysis of phonon–phonon scattering [30] in homogeneous bulk samples implies that normal processes guarantee the drift form of the phonon distribution. The Umklapp processes are taken into account in perturbation theory under the assumption that the inequality $l_U \gg l_N$ is satisfied (where l_U and l_N are the scattering lengths of the Umklapp and normal processes).

Calculating $N(\boldsymbol{k})$ for the point contact is a spatially inhomogeneous problem, and the homogeneous drift solution is inapplicable at least until the condition $l_N \ll d$ satisfied, which is possible only for 'large' point contacts ($d > 10^3$ nm) for $T > \Theta_D/5$.

In the case of weak phonon–phonon scattering in the point contact, the correction to the ballistic thermal conductivity $\dot{Q}^{(0)}$ has the form

$$\dot{Q}^{(1)} = -\dot{Q}_B\left[\frac{d}{l_N^c} + \frac{d}{l_U^c}\right]. \tag{13}$$

The expressions for the point-contact scattering lengths l_N^c and l_U^c contain K-factors depending on the directions of the phonon group velocities, which imposes additional (as compared to the case for the bulk sample) limitations on the type of scattering process [31].

For this reason, the decomposition process $\mathrm{T}'' \Rightarrow \mathrm{T} + \mathrm{T}'$ involving long-wavelength phonons, which is permissible in the bulk material, is not possible in the point contact (here and below, T and L denote the transverse and longitudinal branches of the phonon spectrum). Normal processes of the type $\mathrm{L} \Rightarrow \mathrm{T} + \mathrm{T}'$, $\mathrm{T} \Rightarrow \mathrm{T}_1 + \mathrm{T}_2$ and $\mathrm{T} \Rightarrow \mathrm{T}' + \mathrm{L}$ make contributions to $\dot{Q}^{(1)}$, since one of the velocity vectors in them can be antiparallel to the other two vectors.

For small temperature differences in the contact, the estimated lengths for normal and Umklapp processes practically coincide with the results for the bulk sample. Since the inequality $l_U \gg l_N$ is satisfied for $T > 10$ K, we can assume that the main contribution to the low-temperature thermal resistance of the point contact comes from normal scattering processes.

In the work [32], NaCl–NaCl point contacts with lower heat conductivity were obtained; in these contacts, there was considerable phonon scattering by lattice distortions (with the characteristic scattering length $l < d$). In this case the inelastic scattering has an effective length estimated as $l_{in} \sim (l l_{\mathrm{ph-ph}})^{1/2}$. Here $l_{\mathrm{ph-ph}}$ is the phonon–phonon scattering length for the undisturbed lattice. For small l, i.e. when $l_{in} \sim d$, inelastic scattering can affect the temperature dependence of the heat flux considerably.

3.4. Phonon transmission through an impurity layer

Some anomalies in point-contact heat conductivities have been interpreted as resulting from the presence of a weakly bonded impurity layer at the point-contact boundary [33–35]. In the presence of an intermediate boundary layer weakly bonded to the contact edges, there can be a resonance heat-transfer mechanism. Such a mechanism can be described in the terms of the 'capillary' theory of phonon transmission through impurity layers which are monatomically thick [34, 35]. Such a system of impurity atoms is characterized by weakly dispersed vibrations of the low-resonance frequency ω_0. Note that the amplitudes of the impurity layer displacements are much larger than those of the contacting media surfaces. The resonant frequency dependence of the phonon energy-transmission coefficient D produces a maximum of the function $F(T_2, T_1)$. The resonance frequency is connected to the position of the temperature maximum T_{max} by the relation $\hbar\omega_0 = 3.89\ T_{max}$.

3.5. Non-linear dynamics of a weak point contact

The experimental data show that the creation of PCs by applying pressure leads to polycontact structure of the contact region when the heat conduction between contacting edges is realized through a number of parallel contacts (see section 5). At the contact interface, in addition to the point contacts with strong coupling, there are a large number of microcontacts with weak coupling. As a model of the weak contact, we consider a nanometre-scale tip on a contact edge surface. This tip can push the opposite contact edge. The phonon propagation causes the tip to vibrate. The tensile force in the tip–opposite-edge interface is caused by the adhesion between the tip and the opposite edge.

The dynamical regime of the system including the tip–plate contact is an area whose theoretical [36–38] and experimental [39–41] study is well developed. The realization of the dynamical regime is controlled by the ratio of the characteristic frequency of the surface vibrators (ω) and the resonance frequency of the tip (ω_R). In the linear regime, the tip acts as the waveguide for the vibrations of the contact edges. If the characteristic acceleration of the contact edge exceeds the acceleration of the tip vibrations, this means that the contact is lost. The motion of the tip in this case is formed by the series of impacts between the tip and the opposite edge. This non-linear regime includes aperiodic 'bouncing' as well as vibrations which are subharmonic relative to the exciting frequency ω.

In the case of the weak contact, the characteristic of the longitudinal low-frequency tip oscillations is $\omega_R \sim \pi u/L$, where L is the length of the tip [18]. The characteristic frequency of the surface vibrations at a temperature T can be estimated as $\omega \sim 2\pi uT/a\Theta_D$ (a is the lattice constant). With the increase of the parameter ω/ω_R, the regime of non-periodic tip bouncing occurs for the weak junctions. This effect should be significant if $T/T_{dif} > 1$.

4. Measurement of the phonon heat flux through a point contact

4.1. The adiabatic method for point-contact heat-flux measurements

A simple method for measuring the heat flux through a dielectric point contact has been presented [42]. Using this method, the heat fluxes through NaCl–NaCl [42, 32, 43] and KBr–KBr [44] point contacts were investigated. A technique based on highly stable point contacts was presented, which involves using metal–dielectric point contacts [33].

The experimental scheme is described in detail in reference [32]. Point contacts were created between two dielectric single crystals (or between dielectric crystals and metallic

tips). The bottom single dielectric crystal was suspended in a vacuum under adiabatic conditions while the top single crystal (or a metallic tip) was glued to a copper flange. This flange was in contact, through a copper heat conductor, with a reservoir filled with liquid helium at a temperature T_1 of 4.2 K. The clamping force of the contact edges, and thereby the contact diameter d of the point contact, could be varied by regulating the clamp externally.

The bottom edge was heated up to a temperature T_2 of approximately 80 K with the help of an electric heater. After the heater was switched off, the cooling curve of the suspended bottom crystal was measured. The time dependence of the bottom crystal temperature $T_2(t)$ was found, and the derivative $\mathrm{d}T_2/\mathrm{d}t$ was calculated as a function of temperature with the help of numerical differentiation. Using the thermodynamic definition of the bottom crystal heat capacity $C(T_2)$, the heat flux $\dot{Q}(T_2, T_1)$ is

$$\dot{Q}(T_2, T_1) = C(T_2)\left(\frac{\mathrm{d}T_2}{\mathrm{d}t}\right). \tag{14}$$

The experimental method described above makes it possible to measure with high sensitivity (<1%) the heat flow through a point contact between dielectrics and between a dielectric and a metal tip. In the latter case the Cu needle was produced by the same method as is used to make the needles for metallic PCs [1].

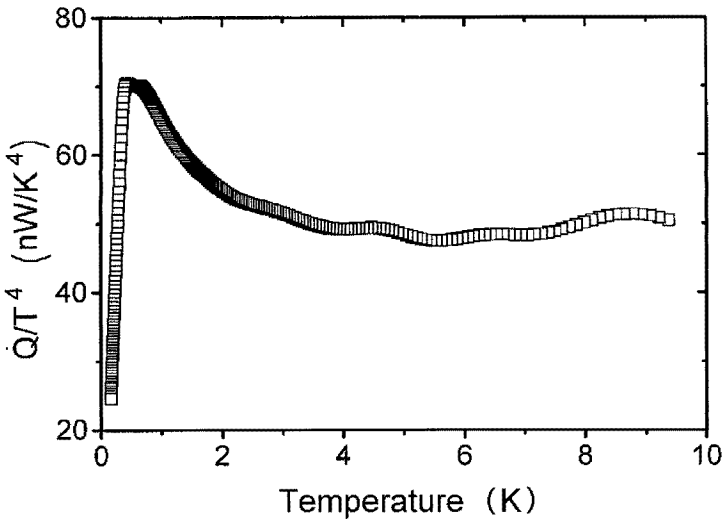

Figure 3. The reduced heat-flux conductivity measured in a Si–Cu point contact. The estimates from the 'spherical flow' model are $d = 30$ nm for the PC diameter and $L/d = 4.5$.

4.2. The low-temperature modification of the anvil–needle technique

In the low-temperature experiments ($T_2 \sim 0.1$ K–10 K), the PCs were made by mounting a single crystal of high-quality Si on three sharp tips, one of which was made of Cu (OFHC), and the other two of Vespel. The heat conductivity of Vespel is very low, and does not contribute to the heat conduction significantly. Similarly, radiation does not provide a significant contribution to the heat conduction. The Cu tip was etched shortly before the PC was formed in order to remove oxide layers. A temperature sensor made from an

NTD-doped natural Ge crystal was glued onto the Si surface with Araldite; the leads were superconducting wires of diameter 50 μm.

The Si crystal was heated up to 10 K using the temperature sensor glued to it. After the heating, the Si crystal was allowed to cooled down by means of the heat flux to the PC formed between the Si surface and the Cu tip. The time dependence of the Si sample temperature was measured, and the heat flux was calculated using the Debye law for heat capacity.

The electrical resistivity of the Si crystals used, at room temperature, was 5 kΩ cm^{-1}. The flat surfaces of Si were cut with a diamond saw. The average surface roughness was 0.7 μm in the case of a surface that was not polished and about 20 Å in the cases of polished surfaces.

5. Experimental results on point contacts

5.1. Heat conductivity in Si–Cu point contacts over the interval 0.1 K–10 K

Figure 3 shows the temperature dependence of the heat flux through a Si–Cu PC over the temperature interval 0.1 K–10 K. This experiment reveals the well-defined peak of the reduced thermal conductivity $F(T_2)$ at $T_{2max} = 0.5$ K. This maximum can be attributed to the diffractional effect. The reduced heat conductivity at the plateau $T_2 > 3$ K is characteristic for phonon transport in the geometrical optics limit. The different peaks at $T_2 > 2$ K demonstrate the polycontact geometry. The estimates from the 'spherical flow' model are $d = 30$ nm for the PC diameter and $L/d = 4.5$ for the contact length.

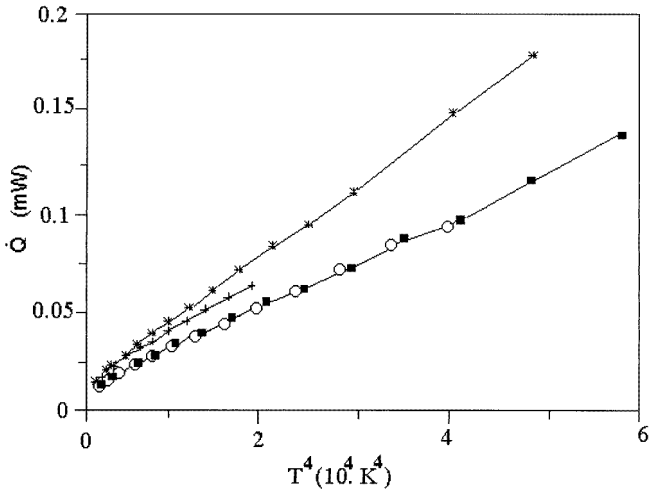

Figure 4. The temperature dependence of the heat flux through Si–Cu point contacts over the temperature interval 4.2 K–20 K, measured by the adiabatic method.

5.2. Heat conductivity through Si–Cu point contacts over the interval 4.2 K–25 K

Figure 4 shows the temperature dependence of the heat flux through a Si–Cu PC over the temperature interval 4.2 K–25 K, measured by the adiabatic method. These contacts are characterized by the ballistic heat condition. It is readily seen that the heat flux represents

a linear function of T_2^4 except in the low-temperature range $T_2 < 10$ K. Estimation based on the geometrical optics model gives a value of the effective PC diameter in the region $d^{(eff)} \sim 5000$ nm. Note that in a polycontact geometry the effective diameter is related to the main diameter of a single contact (d) as $d^{(eff)} = d\sqrt{N}$. Here N is the number of single contacts in a polycontact.

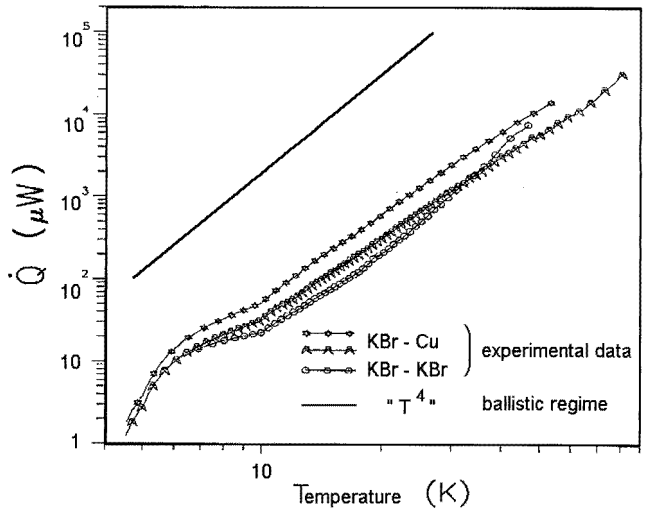

Figure 5. The temperature dependence of the heat flux through KBr–KBr and KBr–Cu point contacts over the temperature interval 4.2 K–25 K, measured by the adiabatic method.

5.3. Heat conductivity through KBr–KBr and KBr–Cu point contacts over the interval 4.2 K–25 K

We investigated more than 50 KBr–KBr and KBr–Cu point contacts by the adiabatic method. KBr single crystals were prepared by the Czochralski method at the Institute of Single Crystals of the Ukrainian National Academy of Science in Kiev. The purity of the samples was 99.99%. The typical data for the temperature dependences of the heat fluxes through KBr–KBr and KBr–Cu point contacts are very similar, and are shown in figures 5 and 6. They indicate a nearly ballistic regime of phonon heat flux for both types of PC over a certain range of temperatures (figure 5).

Deviations from the ballistic heat flux are made clearer when the data are plotted in reduced coordinates (figure 6). The first deviation is the significant monotonic reduction of the PC heat conduction over the temperature region $T_2 > 10$ K. This reduction is evidence of strong phonon scattering in the diffusive regime of the phonon transport. The temperature dependence of the phonon scattering length (l) is estimated to be a power law $l(T_2) \cong T_2^{-s}$, where s varies in the range $0.5 < s < 0.7$. Such a weak temperature dependence is typical of phonon scattering due to statistical strain fields of dislocations [45]. In view of the fact that all of these contacts were obtained by the nail-and-anvil technique, the emergence of stress fields in the contact region seems natural. Secondly, the heat conductivity in reduced coordinates shows a low-temperature maximum at $T_2 = 5.7 \pm 0.2$ K. This anomaly is similar to that observed by Koestler *et al* [46]. The possible connection of this anomaly with resonant transport through layers of weakly bound impurities was discussed in [33–

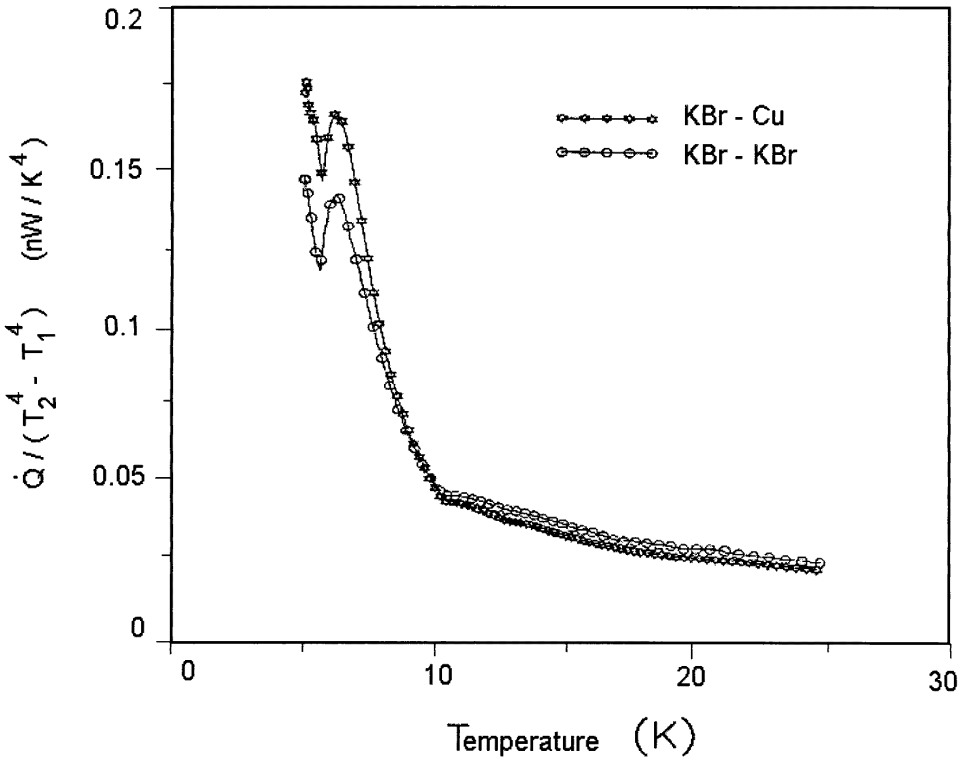

Figure 6. The temperature dependence of the reduced heat flux through KBr–KBr and KBr–Cu point contacts over the temperature interval 4.2 K–25 K.

35]. This anomaly is highly reproducible and has similar features for KBr–KBr and KBr–Cu point contacts. Thirdly, the strong temperature dependence of the reduced heat flux over the interval 5 K $< T_2 <$ 10 K is thought to be due to the intensive Raleigh scattering of low-frequency phonons.

6. Discussion

The specific character of the transport phenomena in point contacts is governed by how easy it is to create a strongly non-equilibrium state of the electron–phonon system in the constriction region. In a traditional treatment like the one discussed in [1], one just applies a potential difference to the edges of the conducting contact. In this case, the electron system usually turns out to be strongly non-equilibrium. The phonon system is slightly excited, to the extent of interacting with electrons to some degree, which is usually rather small in the contact. The situation can be significantly changed if, in addition to a voltage being applied, the edges are kept at different temperatures. If a temperature difference is established across the contact, the phonon system becomes strongly non-equilibrium, too.

The first investigations of non-equilibrium phonon systems in metallic point contacts were connected with the phonon generation in the contact region [48]. Non-equilibrium phonons emitted by electrons in the current-carrying state may be reabsorbed in the contact. The ‘heating’ of phonons in the point contact results in non-spectral corrections to the

current–voltage characteristics—in particular, to the background in the point-contact spectra [7]. Non-equilibrium phonons lead to the specific frequency dependence of the non-linear part of the contact conductivity.

The relaxation of electrons, accelerated in the applied voltage, leads to the establishing of an effective temperature of the phonon system and to the appearance of directed flow of non-equilibrium phonons in symmetrical conducting contacts [49–52]. The consequence of this is analogous to the Peltier effect: at the edges of the symmetrical homogeneous point contact, a difference of temperatures arises, which depends non-linearly on the applied voltage. The concrete nature of this dependence is connected with the contribution of Umklapp processes to the phonon–electron scattering.

A point heat source causes the deviation of the temperature from the equilibrium value of the thermostatically controlled edges. The temperature is determined away from a point contact at distances where relaxation of non-equilibrium electrons and phonons takes place. If we consider the temperature distribution in this region, the point contact can be regarded as a point source of heat. At low temperatures, the phonon scattering length in the contact region may become longer than the distance between the point contact and the point at which the temperature is measured. In this case, the temperature is not a well-defined quantity. This case is considered in detail in [53]. The peaks of the temperature dependence [51, 52] can be caused by the effective thermalization of the phonons with maximal frequency.

It can be concluded that the ballistic phonon transport is realized in dielectric point contacts as well as in point contacts between a metal and a dielectric. It is shown that the phonon thermal conductivity of a contact satisfies a formula analogous to Landauer's formula for electron conductivity. However, the emergence of diffraction effects is determined by the conditions of interaction of elastic waves with the crystal surface.

The analysis of point-contact heat conductivity shows that the suppression of phonon–electron scattering within a PC permits one to use a metallic edge to investigate the phonon transport. The resulting experimental results were reproducible. Experimental heat-flux investigations on KBr–KBr and KBr–Cu PCs demonstrate that the point-contact phonon scattering is determined by the subsurface lattice distortions in dielectric crystals. Investigation of the thermal conductivity of a point contact will certainly give unique information about the state of the crystal surface. Future work should be directed toward obtaining a contact with a controllable structure. 'The Kapitza effect is still filled with surprises' [47], and similar consideration can be applied to the phonon transport in point contacts.

Acknowledgments

We wish to thank M Reiffers, I O Kulik, I K Yanson, H van Kempen and J M van Ruitenbeek for helpful discussions. We should like to thank R Mlýnek for helpful assistance. The work of one of us (AS) was facilitated by the support of the International Science Foundation. The work was partially supported by Slovak VEGA grants Nos 1/4385/97 and 2/4176/97.

References

[1] Duif A M, Jansen A G M and Wyder P 1989 *J. Phys.: Condens. Matter* **1** 3157
[2] Sharvin Yu V 1965 *Sov. Phys.–JETP* **21** 655
[3] Yanson I K 1974 *Sov. Phys.–JETP* **39** 506
[4] Kulik I O, Omelyanchouk A N and Shekhter R I 1977 *Sov. J. Low Temp. Phys.* **3** 740
[5] Jansen A G M, Mueller F M and Wyder P 1977 *Phys. Rev.* B **16** 1325

[6] Yanson I K 1983 *Fiz. Nizh. Temp.* **9** 676
[7] Reiffers M and Samuely P 1990 *PHONONS 89* ed S Hunklinger, W Ludwig and G Weiss (Singapore: World Scientific) p 1293
[8] Muller C J, van Ruitenbeek J M and de Jongh L J 1992 *Physica* C **191** 485
[9] van Kempen H and Shklyarevskii I O 1993 *Sov. J. Low Temp. Phys.* **19** 150
[10] Bogachek E N and Shkorbatov A G 1985 *Sov. J. Low Temp. Phys.* **11** 353
[11] Little W A 1959 *Can. J. Phys.* **18** 334
[12] Weis O 1984 *Phonon Scattering in Condensed Matter* ed M Meissner and R O Pohl (Berlin: Springer) p 179
[13] Khalatnikov I M 1952 *Zh. Eksp. Teor. Fiz.* **22** 687
[14] Swartz E T and Pohl R O 1989 *Rev. Mod. Phys.* **61** 605
[15] Kapitza P L 1941 *Zh. Eksp. Teor. Fiz.* **11** 1
[16] Young D A and Maris H J 1989 *Phys. Rev.* B **40** 3685
[17] Štefányi P, Fozooni P, Lea M J, Saunders J, Feher A, Zaboj R and Shkorbatov A G 1993 *Phonon Scattering in Condensed Matter VII* ed M Meissner and R O Pohl (Berlin: Springer) p 156
[18] Shkorbatov A G, Sarkisyants T Z, Feher A and Štefányi P 1993 *Sov. J. Low Temp. Phys.* **19** 881
[19] Landauer R 1987 *Z. Phys.* B **68** 217
[20] Morse P M and Feshbach 1953 *Methods of Theoretical Physics* (New York: McGraw-Hill)
[21] Zagoskin A M and Kulik I O 1990 *Sov. J. Low Temp. Phys.* **16** 911
[22] Bouwkamp C J 1941 Theoretische en numereke Behemdelung van de buiging Door een ronde Opening *Dissertation* University of Groningen
[23] Levine H and Schwinger J 1948 *Phys. Rev.* **74** 958
[24] Levine H and Schwinger J 1949 *Phys. Rev.* **75** 1423
[25] Torres J A, Pascual J I and Saenz J J 1994 *Phys. Rev.* B **49** 16 581
[26] Scherbakov A G, Bogachek E N and Landman U 1996 *Phys. Rev.* B **53** 4054
[27] Torres J A and Saenz J J 1996 *Physica* B **218** 234
[28] Kehraskos D 1990 *J. Phys.: Condens. Matter* **3** 1443
[29] Kulik I O, Shkorbatov A G and Feher A 1998 *Sov. J. Low Temp. Phys.* at press
[30] Gurevich V L 1986 *Transport in Phonon Systems* (Amsterdam: North-Holland) p 418
[31] Shkorbatov A G and Sarkisyants T Z 1990 *Sov. J. Low Temp. Phys.* **16** 427
[32] Štefányi P, Feher A and Shkorbatov A G 1992 *Sov. J. Low Temp. Phys.* **18** 107
[33] Feher A, Štefányi P, Zaboj R, Shkorbatov A G and Sarkisyants T Z 1992 *Sov. J. Low Temp. Phys.* **18** 373
[34] Syrkin E S, Sarkisyants T Z and Shkorbatov A G 1993 *J. Phys.: Condens. Matter* **5** 5059
[35] Syrkin E S, Shkorbatov A G and Feher A 1993 *Phonon Scattering in Condensed Matter VII* ed M Meissner and R O Pohl (Berlin: Springer) p 421
[36] Pippard A B 1978 *The Physics of Vibration I* (Cambridge: Cambridge University Press)
[37] Hirdmarsh M B and Jeffries D J 1984 *J. Phys. A: Math. Gen.* **17** 1791
[38] Foale S 1994 *Proc. R. Soc.* A **347** 353
[39] Kolosov and Yamanaka 1993 *Japan. J. Appl. Phys.* **32** 1095
[40] Rabe U and Arnold W 1994 *Appl. Phys. Lett.* **64** 1493
[41] Burnham N A, Kulik A J, Gremaud G and Briggs G A D 1995 *Phys. Rev. Lett.* **74** 5092
[42] Štefányi P, Feher A and Orendacova A 1990 *Phys. Lett.* **143** 259
[43] Štefányi P and Feher A 1990 *Physica* B **165+166** 911
[44] Feher A, Štefányi P, Zaboj R and Shkorbatov A G 1993 *Phonon Scattering in Condensed Matter VII* ed M Meissner and R O Pohl (Berlin: Springer)
[45] Wybourne M N and Wigmore J K 1988 *Rep. Prog. Phys.* **51** 923
[46] Koestler L, Wurdack S, Dietsche W and Kinder H 1986 *Phonon Scattering in Condensed Matter V* ed M Meissner and R O Pohl (Berlin: Springer) p 171
[47] Meissner M and Pohl R O 1992 *Condens. Matter News* **1** 3
[48] Kulik I O 1985 *Sov. J. Low Temp. Phys.* **11** 516
[49] Bogachek E N, Shkorbatov A G and Kulik I O 1989 *Sov. J. Low Temp. Phys.* **15** 156
[50] Bogachek E N, Kulik I O and Shkorbatov A G 1991 *J. Phys.: Condens. Matter* **3** 8877
[51] Reiffers M, Flachbart K and Janos S 1986 *JETP Lett.* **44** 389
[52] Reiffers M and Flachbart K 1987 *Japan. J. Appl. Phys. Suppl.* 3 **26** 649
[53] Katerberg J A, Reynolds C L Jr and Anderson A C 1977 *Phys. Rev.* B **15** 673